Energy & Buildings 275 (2022) 112474

Contents lists available at ScienceDirect

Energy & Buildings

journal homepage: www.elsevier.com/locate/enb

Modelling and real-data validation of a logistic centre using TRNSYS®: Influences of the envelope, infiltrations and stored goods

F. Vera-García [a], J.J. Rubio-Rubio [a], A. López-Belchí [b], E. Hontoria [c,*]

[a] Thermal and Fluids Engineering Department, Technical University of Cartagena, Doctor Fleming s/n, 30205 Cartagena, Murcia, Spain
[b] Engineering and Applied Techniques Department, University Centre of Defense at the Spanish Air Force Academy, San Javier Air Base, 30729 Santiago de la Ribera, Murcia, Spain
[c] Business Economics Department, Technical University of Cartagena, Spain

ARTICLE INFO

Article history:
Received 2 June 2022
Revised 30 August 2022
Accepted 10 September 2022
Available online 20 September 2022

Keywords:
TRNSYS
SKETCHUP
Infiltrations
Thermal Load
Case Study
Perishable product refrigeration

ABSTRACT

In this paper, the authors aim to support users when modelling scenarios with complex processes entailing thermal loads and infiltrations. The large building analysed is a logistics centre for the replenishment and distribution of perishable foodstuffs where cold chains must be maintained. The logistics centre, with 96 loading/unloading docks, handles large turnovers of different goods. This produces heat inside the facility. Due to continuous loading/unloading, the infiltrations in the building, and the fixed and variable thermal loads, this facility consumes a large amount of energy.

Aiming to optimise the centre and contribute to sustainable development goal SDG7, this building has been modelled with a classical non-D envelope using TRNBuild® and also with the more sophisticated 3D software, SketchUp®, to compare and validate their results over a year with real consumption, as well as to assess the main sources of energy consumption. To obtain reliable results, the authors provide some methodology models to identify the sources of the building's thermal losses and quantify the different sources of consumption. These models are useful tools to support decision-makers (to improve insulation and arrange loads, among other things) when trying to reduce energy use in large buildings with intense operating processes.

The results indicate that by modelling the entire facility with 3D software, the model estimation differs from real consumption by around 7.22%, while using a non-D model increases the difference to 26%. Additionally, the results show that around 47% of the energy consumption in the building is due to air infiltrations during loading/unloading, 18% is due to perishable products, and around 30% is due to building insulation. The methodology and models presented here, including the possibility of modifying the thermal load profiles, have demonstrated their capacity to reduce and optimise the load demand of refrigeration for warehouses if reliable data records are available.

1. Introduction

Energy consumption in buildings represents a large percentage of worldwide energy use. In the European Union, buildings account for 40 % of total energy consumption [1]. In the rest of the world, the percentage is similar [2]. Moreover, the energy used by Heating, Ventilation and Air Conditioning (HVAC) systems varies from 16 to 50 % of the total energy consumed in buildings around the world [3], and they produce 33 % of the world's greenhouse gas emissions [4]. In our current competitive and global market, there is growing concern over greenhouse gas emissions and global warming. Policymakers and businesses are increasingly focusing on energy efficient buildings and reducing operational energy consumption [5]. Policies designed to cut energy consumption and gas emissions are generally based on three main actions: (i) optimising the energy use of technical edifice systems, (ii) reducing energy loss through the building envelope and (iii) promoting the use of energy from renewable sources.

To achieve efficient systems, some tests to assess their impact on the thermal behaviour of buildings should be undertaken. However, due to reasons like not wanting to interrupt daily work, needing to preserve perishable goods or the impossibility of making large investments, these tests are not viable options. To address these drawbacks, the importance of modelling and simulation is unquestionable. Software analysis lets the user develop a virtual model to perform analyses that would not otherwise be possible. For building modelling, different types of software are available.

* Corresponding author.
E-mail address: eloy.hontoria@upct.es (E. Hontoria).

https://doi.org/10.1016/j.enbuild.2022.112474
0378-7788/

Nomenclature

a_d	Area of each dock in m^2
$a_{l/u}$	Area of the gap in the non-hermetic dock in m^2
a_t	Number of trucks that arrive to the warehouse daily
AHRG	Average Heat Released by the Goods stored in the warehouse in $W{\cdot}kg^{-1}$
B	Coefficient related with the space set aside for corridors and machinery in the warehouse
GPL	Gross Product Load in $kg{\cdot}m^{-2}$
HRMAG	Heat Released by the Maximum Amount of Goods stored in the warehouse in W
k_{goods}	Constant which averages the heat released per kilogram of goods stored in the warehouse in $W{\cdot}kg^{-1}$
$k_{l/u}$	Constant to calculate the air infiltration flow rate during the loading and unloading process in $m^2{\cdot}sec{\cdot}h^{-1}$
$k_{parking}$	Constant to calculate the air infiltration flow rate during the time a truck is parked in $m^2{\cdot}sec{\cdot}h^{-1}$
$k_{storage}$	Coefficient representing storage density of warehouse
NMAG	Net Maximum Amount of Goods stored in the warehouse in kg
NPL	Net Product Load in $kg{\cdot}m^2$
TAW	Total Area of the Warehouse in m^2
$\dot{q}$	Air infiltration flow rate in $m^3{\cdot}h^{-1}$
$t_{l/u}$	Time spent loading or unloading one pallet in *sec*
t_p	Time a truck spends parked in the dock in *sec*
UAW	Useful Area of the Warehouse in m^2
v_{wind}	Wind velocity in $m{\cdot}sec^{-1}$

Most of them let the user define, simulate and optimise the design of the building in terms of energy consumption. TRaNsient System Simulation Tool (TRNSYS®) is one of the most frequently used software products among the research community since it offers the possibility to include models defined by the user.

Although TRANSYS has been widely used to model buildings (see literature review in Section 2), few works have dealt with calculating the accuracy of the results when using basic structural elements incorporated into TRNSbuild® (non-D model) or doing a more demanding modelling (3D modelling) with SketchUp®. Albeit the non-D model has high quality to predict the thermal demand of a building, the 3D model allows users to incorporate geometric aspects to define specific internal heat flows, which can be later exported to TRNSYS®. This permits more accuracy to be obtained in the real demand due to the building's envelope. It is worth noting that the 3D model explained in this work does not involve making a Computational Fluid Dynamic (CFD) model of the building to calculate thermal demand.

To show how great the differences can be, the envelope design was modelled using both methods, and the results were validated by comparing them to a year's real energy consumption in the building.

2. Literature review

TRNSYS® is sophisticated energy simulation software that has been widely used to optimise buildings. Some examples of the use of TRNSYS® software in the open literature are Massaguer et al. [6], who developed a new TRNSYS® type for the simulation of thermoelectric generators and validated the new type of component under transient and steady-state conditions. Comparing the model results and the experimental data showed errors of less than 4 % for temperature differences between cold and hot sides and electrical output power. Quesada et al. [7] proposed a dynamic model of a 7.2 kWp photovoltaic installation to accurately predict the long-term performance of the installation. To obtain a model representing real installation reliably, they address several modifications of standard test conditions. Webb et al. [5] simulated a biomimetic façade using TRNSYS® to improve the thermal performance of the building façade based on biological models of animal fur and blood perfusion. They reduced energy consumption by up to 17 % compared to conventional approaches using biomimetic principles combined with a mathematical model in a commercial office building in Melbourne.

Kenai et al. [8] implemented a dynamic thermal simulation of a residential building in an urban environment to analyse the effect of a green wall of Virginia Creeper using TRNSYS®. With the green walls, they reduced air conditioning requirements in summer. As this plant is deciduous, the façade was exposed in winter and could absorb solar radiation.

Eddib et al. [9] studied the hydro-thermal behaviour of a multizone apartment located in northern Morocco to estimate the air conditioning and heating requirements during summer and winter. Since Morocco imports over 96 % of the energy that it consumes, the energy-based rehabilitation of residential buildings is a promising field.

Potočnik et al. [10] used TRNSYS® to investigate how to increase thermal comfort in residential buildings by using smart controls and the optimisation of weather-controlled air-to-water heat pumps based on a predicted mean vote thermal comfort model. As a result, they considerably improved thermal conditions by adding factors that affect machine operations, such as solar radiation.

Sarbu and Pacurar [11] experimentally and numerically studied indoor environmental quality in university classrooms using subjective and experimental measurements in air-conditioned classrooms. They provided a prediction model of academic performance, finding that student performance was affected by indoor environmental conditions.

Delgado et al. [12] proposed an adaptative control model using TRNSYS® to adjust and optimise the heat input from solar collectors or backup boilers to maximise solar input in an indoor public swimming pool. Their results indicate that the predictive controls obtained from these kinds of models can reduce swimming pool energy use by 18.76 %. Delcroix et al. [13] modelled phase change material in building envelopes to create a wall with variable properties. Their model focused on the effect of spatial and temporal discretisation on the performance of the model, and it was validated using wall test cases proposed by the International Energy Agency.

TRNSYS® can also be used to develop economic analyses or even specific heat exchangers, as published by Villa-Arrieta and Sumper [14] and Brough et al. [15], respectively. Villa-Arrieta and Sumper [14] presented a technical–economic model to evaluate energy systems, coupling TRNSYS® with technical simulation software. The economic calculation was performed according to the Energy Performance of Buildings Directive of the European Commission. As a result, they provide a tool to evaluate the consumption of communities from a technical point of view.

Regarding phase change systems, Bordignon et al. [16] developed a novel model for TRNSYS® to simulate a reversible water-to-water heat pump based on the polynomials of the compressor's characteristic curves, linked with Refprop®, to evaluate the properties of refrigerants. This new model was used to analyse a ground source heat pump in a historic building. Brough et al. [15] proposed a new model to simulate heat pipe heat exchangers for waste heat recovery. Using this model, the authors obtained a reduction in emissions, as well as potential savings when using this system to recover energy.

Although the authors have focused their efforts on the modelling of the logistic centre using the TRNSYS software and an ulterior improvement of the envelope design trough SketchUp®, both of them could have been integrated in BIM technology that is shortly explained in the next section.

2.1. Building information modelling (BIM) to estimate thermal loads

BIM technology supports the study and analysis when addressing a 3D digital building model with the aim of obtaining a virtual equivalent of the buildings.

Several works may be found in the literature review which have tackled the thermal loads of a building applying this software, but most of them are regarding the design phase. In [17] the authors reduce the load on the HVAC by 81.8 % using this program and analysing the most adequate façade and its orientation. Also, in [18] is presented a framework where the algae façade is integrated in BIM as one of the components.

Dealing with control strategies, in [19], the authors based the research on BIM data to automatize the generation of control strategies for a building heating system. Additionally, a BIM-based workflow is proposed in [20] where Building Envelope Trade-off Method (BETM) is used in the early design phase.

However, and as a result of the literature review, few works (if any) have integrated TRNSYS® and SketchUp® into Building Information Modelling which could be a first step for future lines of research.

3. Logistic centre building

In this section, some features of the analysed logistic centre, namely, its location, building characteristics, daily operating processes, and cooling system, are described.

3.1. Location

The industrial warehouse is located in the Region of Almeria, in southeastern Spain. This area has a warm climate, with average annual temperatures ranging between 17 and 18 °C. Atlantic wet fronts bring precipitation when they hit the Betic Cordillera. Rain usually falls in torrents for a few days in the fall or spring, and the area has very dry summers. Winters are usually mild, with mean temperatures below 9 °C. Summers are hot, 31–32 °C are the typical maximum temperatures in July and August, although temperatures sometimes exceed 40 °C. Due to the size and topographical variability of the municipality, not all areas report the same rainfall and temperatures.

If TRNSYS® does not have exact weather data about a specific area, this information must be gathered from the the closest areas and afterwards entered into TRNSYS®. In our work and during the analysed year, the temperature generally varied from 4 °C to 33 °C, and it rarely dropped below 0 °C or rose above 36 °C. Real outdoor temperature data throughout one year were recorded and compared with the same values from the TRNSYS® database, Fig. 1.

The model has been developed to obtain an average value for the demand over a standard year. Therefore, the average climatic data of the area where the warehouse is located are used as input variables. Fig. 1 shows only the comparison between the temperature measure collected during a year and the temperature from the database used with TRNSYS®. But it is important to note that for the correct behaviour of the model, the authors have implemented all the parameters of the environmental conditions as input variables: dry and wet bulb temperature, direct and diffuse radiation, rain, humidity, etc. The weather data are taken from the meteorological database Meteonorm in TRNSYS®.

Since the outdoor temperature is higher than the warehouse's setpoint inside temperature almost all year, the modelling of the building must be as accurate as possible to obtain adequate upgrades in the refrigeration system.

3.2. Industrial warehouse

The internal dimensions of the industrial warehouse are: 276 m long, 54 m wide, and 9.50 m high. It is divided into two areas, one with a setpoint temperature of 8 °C and the other set at 4 °C. The useable surface of each area is 13.456 m^2 and 1.414 m^2, respectively.

The thermal envelope was built with the following construction elements:

- Concrete wall 1.15 m high from the ground.

- Vertical walls built with 32-centimetre-thick precast concrete from the concrete wall to 5.85 m high and from 5.85 m high to the roof with a 10-centimetre-thick sandwich panel.

- The loading docks are 9 square metres and were built with a 7-centimetre-thick sandwich panel.

- There are sixteen skylights located on the roof.

- The 320-millimetre-thick gabled roof has several layers of insulation.

The 4 °C area is divided into three zones: a loading aisle, an unloading aisle, and a chamber separated from the aisles by sandwich-panelled walls where the goods are stored.

The layers of the walls, ceiling, and roof and the thermal transmittance of each part obtained from TRNSYS® are as follows:

- Precast concrete: reinforced concrete (10 cm), XPS (10 cm), reinforced concrete (10 cm). U_1 = 0,305 $W{\cdot}m^{-2}{\cdot}K^{-1}$.

- Sandwich panel of external walls: steel (1 mm), rock wool (10 cm), steel (1 mm). U_2 = 0,375 $W{\cdot}m^{-2}{\cdot}K^{-1}$.

- Sandwich panels of the rest of the walls: steel (1 mm), PUR (7 cm docks, 30 cm roof, 10 cm internal walls), steel (1 mm). U_{docks} = 1,923 $W{\cdot}m^{-2}{\cdot}K^{-1}$. U_{roof} = 0,855 $W{\cdot}m^{-2}{\cdot}K^{-1}$. $U_{internal\ walls}$ = 1,492 $W{\cdot}m_{-2}{\cdot}K^{-1}$.

- Floor of the 8 °C chamber: reinforced concrete (18 cm), XPS (10 cm), stone (30 cm). U_3 = 0,292 $W{\cdot}m^{-2}{\cdot}K^{-1}$.

- Floor of the 4 °C chamber: reinforced concrete (18 cm), LDP (10 cm), reinforced concrete (20 cm), polypropylene (20 cm), reinforced concrete (5 cm), stone (30 cm). U_4 = 0,582 $W{\cdot}m^{-2}{\cdot}K^{-1}$.

The properties of each material are shown in Table 1.

3.3. Perishable goods and operational processes

According to the annual reports provided by the company, the amount of goods (mainly fruit and vegetables) the warehouse handles is around 2.5 million tons every year, stored according to perishability, as shown in Fig. 2. The large differences in quantity stored in peak and low seasons can also be seen. From October to February, there are 25 % more goods stored in the warehouse. This is because the main product the company transports is berries, which are winter season products.

To preserve the quality of the perishable products as much as possible, the goods are not stored more than twenty-four hours in the warehouse. This is why the facility is running 24 h, 7 days a week (Fig. 3 and Fig. 4), with the 24th hour equalling 00:00 h. An average of 313 trucks load and unload goods daily. Products are combined in the warehouse (cross docking) to fill a truck with various products that will be delivered to customers in different

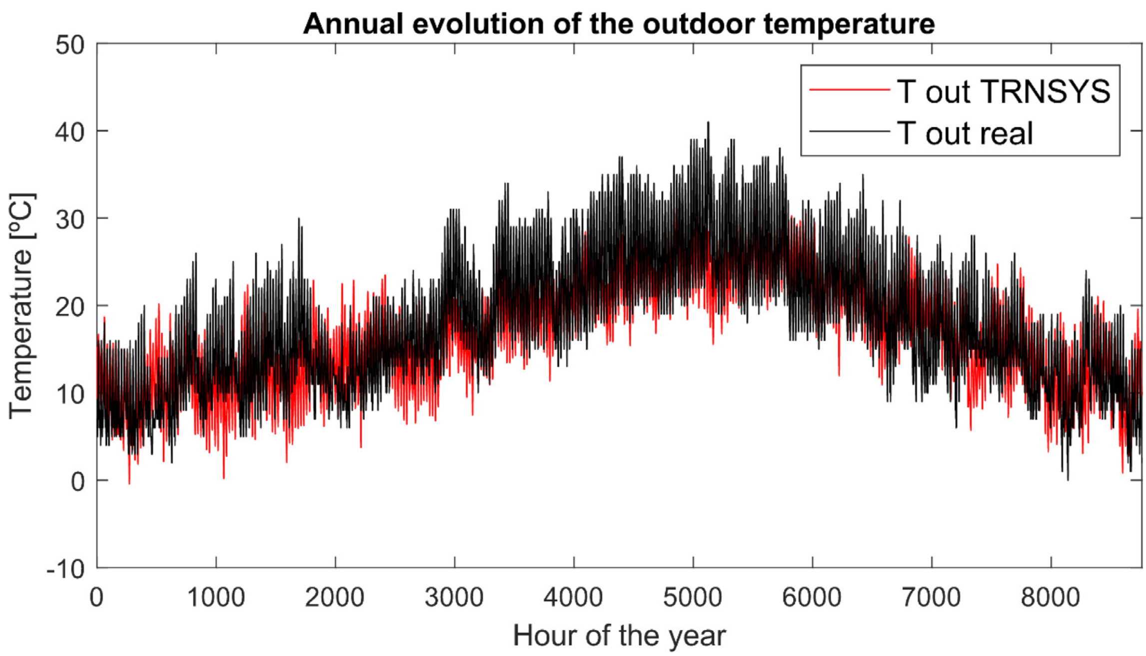

Fig. 1. Annual evolution of the outdoor temperature in TRNSYS®.

Table 1
Properties of materials used in the building envelope.

Material	Thermal conductivity $Wm^{-1}K^{-1}$	Heat capacity $Jkg^{-1}K^{-1}$	Density kgm^{-3}
Rock wool	0.39	839	31
Reinforced concrete	2.33	1,003	2,401
LDP	0.34	2,202	918
XPS	0.29	1,449	33
Polyproplyene	0.21	1,799	911
PUR	0.22	1,502	41
Stone	2.03	1,052	1,451
Steel	50.03	448	7,799

parts of Europe. This is the daily modus operandi of the company, and it implies continuous opening of the loading/unloading docks. As a consequence, infiltrations throughout the day, along with heat released by different goods, make it difficult to achieve an accurate model of this specific warehouse.

The amount of goods that are loaded and unloaded per hour in the warehouse on a typical day is represented in Fig. 3, where the obstacles to obtaining a feasible model can be seen.

Because of the significant number of trucks that arrive daily to load and/or unload goods, a study of the existing infiltrations (see Fig. 4) is needed to assess the systeḿs performance. At this point, it is worth noting that more trucks are in the warehouse at the hottest time of the day (12:00–13:00), as Fig. 4 shows. This obviously increases energy consumption.

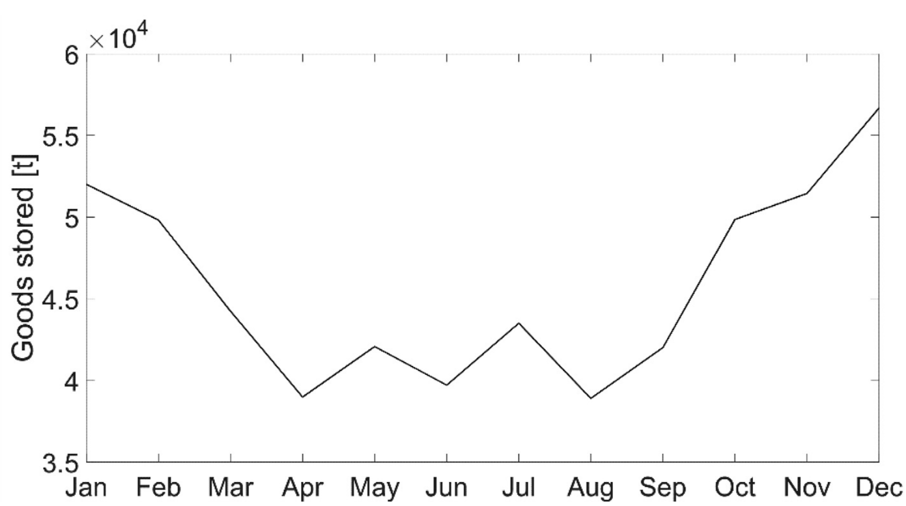

Fig. 2. Goods stored in the warehouse each month.

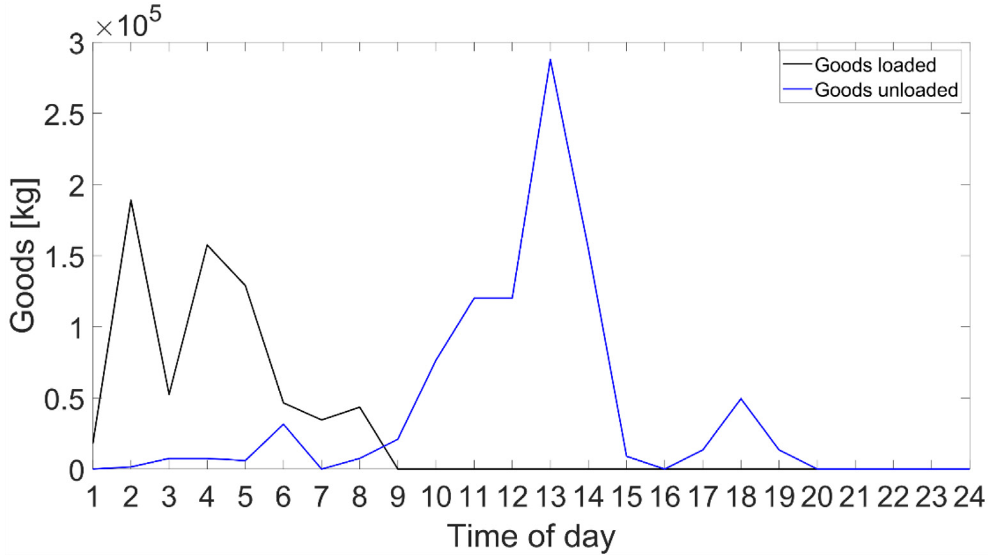

Fig. 3. Tons of goods loaded and unloaded on an hourly basis.

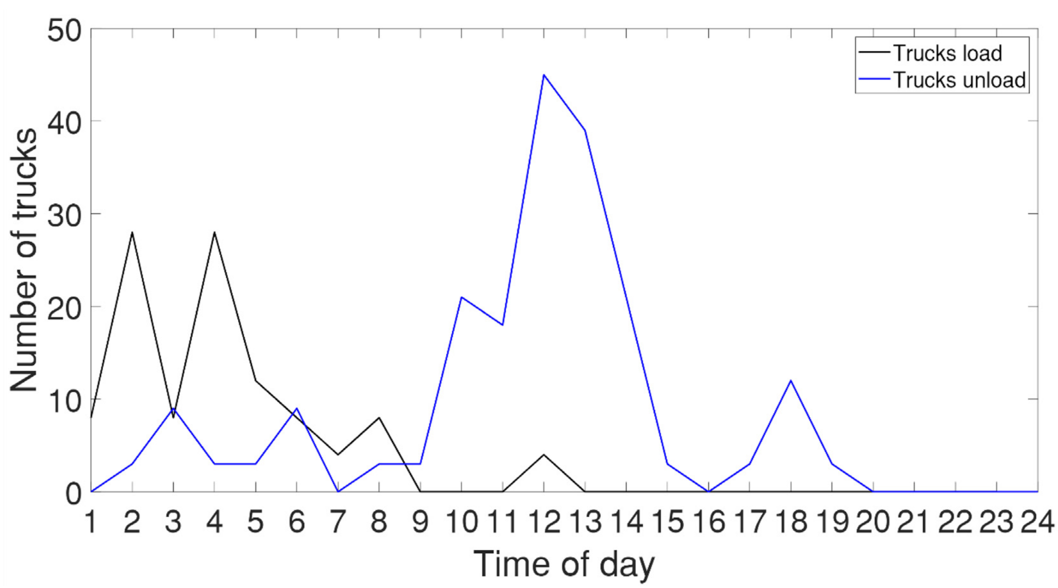

Fig. 4. Daily number of trucks loading and unloading.

As explained above, another key factor regarding energy consumption is the thermal load generated by the heat released from the different perishable goods. Since it is complex to gauge the energy consumption involved in this issue, a specific methodology to do so is presented in Section 5 (Fig. 9).

4. Description of the cooling system

To achieve proper conditions in the chambers, there is a cooling system with two R134a chillers used to cool a propylene glycol heat transfer fluid. This mixture is pumped through the pipe network to the coils located throughout the warehouse, where the heat exchange with the air inside the chambers takes place. Once the mixture is heated in the heat exchangers, it is returned to the chillers. Therefore, it is a closed indirect cooling system. The basic design of the cooling system is presented in Fig. 5.

The operating principle of each chiller is as follows. The refrigerant enters the compressor in a gaseous state at low pressure and is then compressed to high pressure. The refrigerant passes through an oil separator before being sent to the condenser, where it becomes liquid. In the condenser, the refrigerant releases the heat into the atmosphere (air acts as a condensing agent). The refrigerant, which is liquid, moves into a liquid container, from where it is distributed to the multitube exchangers and evaporates, decreasing the temperature of the evaporating agent (propylene glycol mixture). Finally, the refrigerant is suctioned by the compressors, closing the mechanical vapor compression cooling cycle.

Besides the two chillers and the pipe network, the cooling system includes twenty-four cooling coils located throughout the warehouse and two pumping groups. The main characteristics of this equipment and the monthly energy production of each chiller have been obtained from the Supervisory Control And Data Acquisition (SCADA) system installed in the warehouse. The main characteristics of the SCADA are shown in Table 2, Table 3 and Fig. 6.

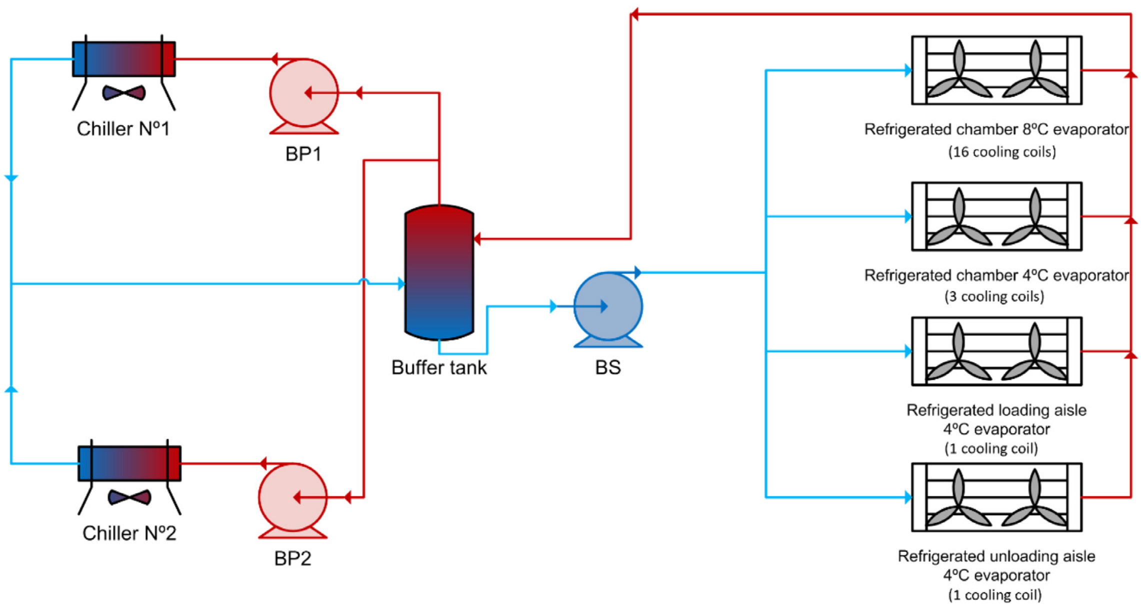

Fig. 5. Design of the cooling system.

Table 2
Air-to-air chiller characteristics.

Cooling Capacity	795.45 kW
Cooling Efficiency (EER)	2.42
Seasonal Efficiency (ESEER)	3.53
Fluid Type	Propylene Glycol (35 %)
Leaving Temperature	−5.0 °C
Entering Temperature	−0.5 °C

Table 3
Main characteristics of the cooling coils.

	Chamber 8 °C	Chamber 4 °C	Loading/ Unloading aisle 4 °C
Cooling Capacity	137.5 kW	50.2 kW	59.4 kW
Temperature air inlet	8 °C	4 °C	4 °C
Outlet air temperature	3.2 °C	1.4 °C	0.7 °C
Inlet fluid temperature	−5 °C	−5 °C	−5 °C
Air flow	49,533 m^3/h	37,254 m^3/h	41,378 m^3/h
Amount	16	3	2

5. Methodology for modelling the complex system

To properly guide researchers and practitioners when modelling complex systems, the methodology presented in Fig. 7 is provided to clarify the research method followed by the authors and also the system modelling to obtain accurate results in this complex scenario.

The methodology supports users in the total assessment of each one of the main sources of consumption and compares them with the total demand of the cooling system to detect discrepancies. Large discrepancies, indicate shortcomings in the calculation of the internal thermal loads, the modelling of the building envelope or both of them.

The methodology starts with data collection. As a consequence of the analysis of the large empirical dataset, two main blocks of consumption are identified. The first one involves the thermal loads inside the building due to operational processes. It has three main factors: (i) the heat released by the goods (Table 4), (ii) air infiltrations due to loading and unloading activities and (iii) the thermal load of internal elements like the machinery, employees, lighting, etc. To address these issues, a procedure is designed in Section 6. The second block of consumption involves the thermal loads of the building envelope. To appraise accurate consumption, a ~~0D~~ non-D and 3D model are presented for their comparison with real consumption demand. Section 7 is devoted to this second block.

Once the total thermal loads have been determined, the first trial is conducted with TRNSbuild® to adjust the building envelope with a basic non-D model. If consumption is close to the real demand of the cooling system, the modelling is considered satisfactory. If not, the modelling of the building envelope must be improved through SketchUp® (3D modelling), and the procedure is carried out again.

In this complex and dynamic scenario, the calculation of the total internal thermal loads of the building requires comprehensive analysis. Due to the difficulty of obtaining reliable and instantaneous data on the thermal loads of the infiltrations and storage goods, a sequential step procedure is required (Fig. 8). This is shown in the following section.

Once the internal loads have been obtained, they are computed with TRNSYS® in both non-D and 3D. The results of this simulation are compared with the data on real energy consumption. If the difference is below 10 %, the model is validated, and no further work is needed. If the difference is 10 % or above, a 3D simulation is performed and checked with real data to assess its feasibility. The 3D simulation with Sketchup® includes the influence of building orientation, among other things.

The results obtained with TRNSYS® and the 3D model are compared with real energy consumption data. This data is used to adjust the models of thermal loads as it́s explained in Sections 6 and 7.

6. Internal thermal loads of the building

Because of the operational processes of the company, two factors have a great impact on the energy requirements of the warehouse: the heat released by the goods stored until they reach a thermal equilibrium with the warehouse (section 6.1) and the air infiltrations during the loading and unloading processes (section

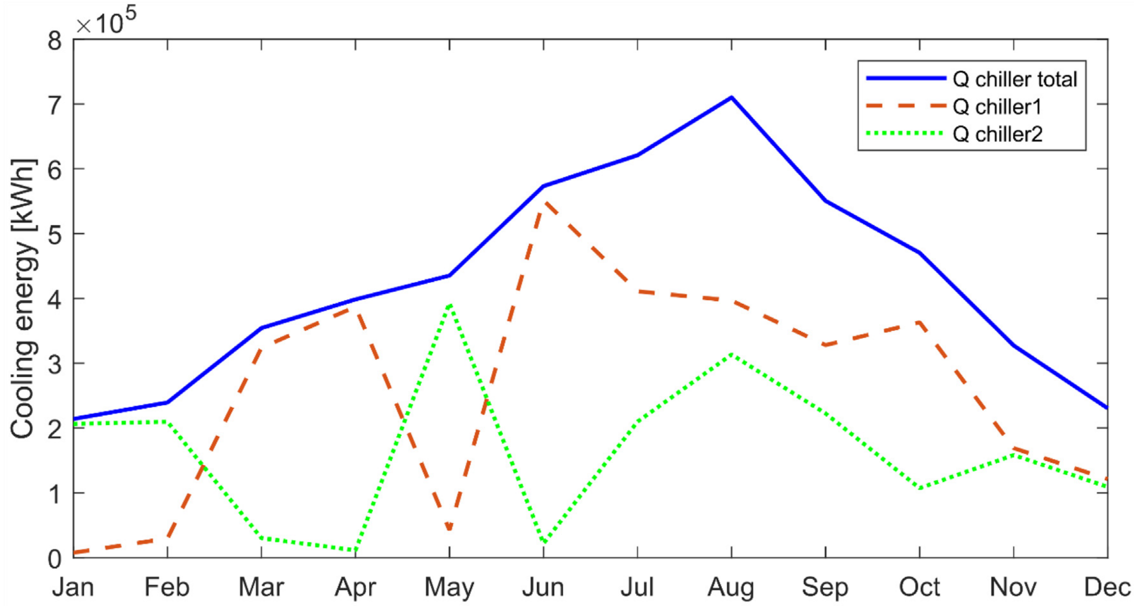

Fig. 6. Monthly energy cooling produced by chillers.

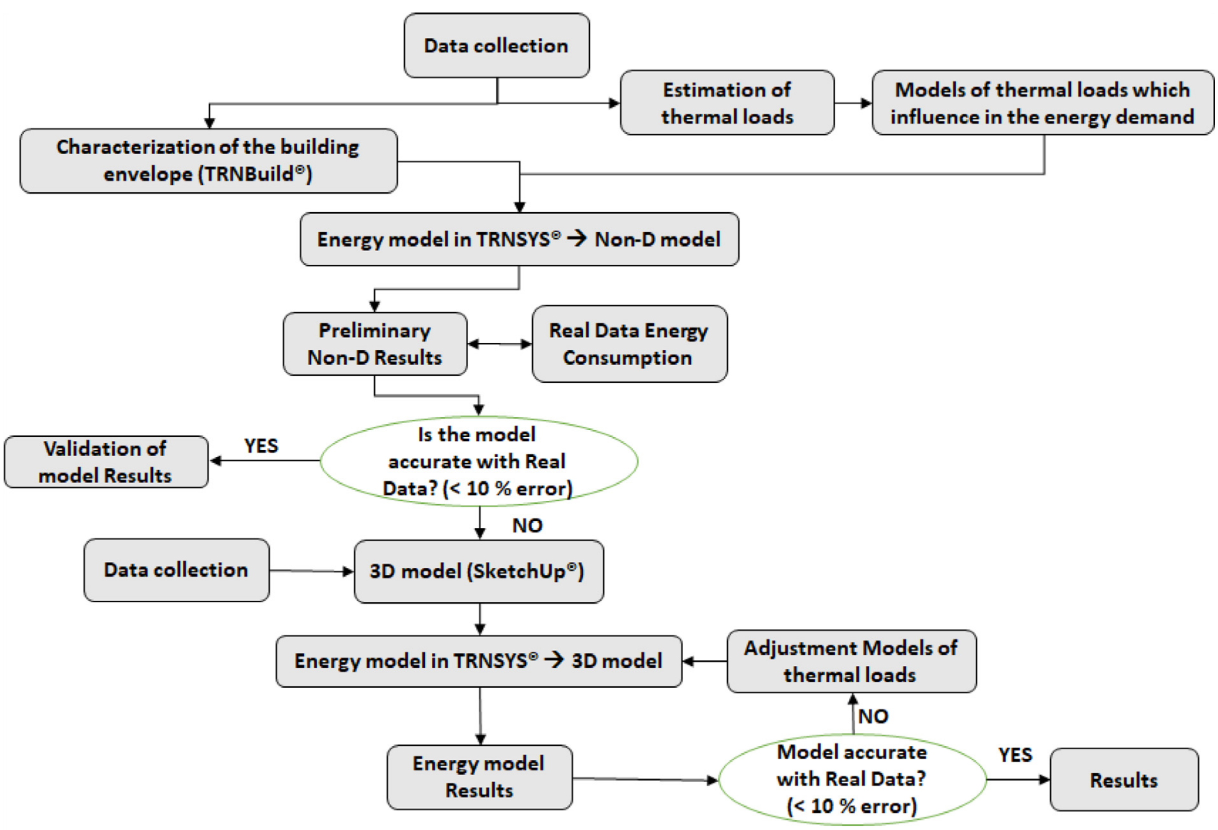

Fig. 7. Methodology to model and refine the system.

6.2). The remaining factor to be taken into account is the thermal load due to internal elements (section 6.3).

6.1. Heat released by the goods stored in the warehouse

Because of the complexity of the company's operational processes, including frequent loading and unloading, it is almost impossible to gauge the exact amount (kg) of any kind of stored product at any given time. For this reason, an average of the power released per kilogram of goods stored must be estimated using information such as the average heat released by fruit and vegetables (most habitually stored), the total surface available for storage and storage density. The detailed procedure of this calculation is shown in Fig. 8.

Table 4
Heat released by the different types of goods stored in the warehouse in kcal/t.

Goods	Temperature [°C]			Annual amount over total goods stored [%]
	0	4.4	15.5	
Celery	450	670	2300	4.32 %
Blueberry	170–200	240–270	400–500	4.80 %
Onion	185–310	490–550	–	3.99 %
Cherry	370–490	–	3000–3700	0.83 %
Cabbage	330	470	1130	0.99 %
Salad	3100	4400	12,800	0.62 %
Spinach	1180–1550	2200–3100	10,500	3.17 %
Raspberry	–	–	4300–4900	5.60 %
Strawberry	700–1050	1400–1800	4300–5300	5.31 %
Pea	2300	3700	11,000	2.82 %
Bean	1500–1700	2500–3200	9000–12000	5.38 %
Lemon	160	225	830	4.26 %
Sweet corn	1800	2600	11,600	3.12 %
Apple	185–280	300–500	1200–1800	2.15 %
Peach	240–380	400–560	2000–2600	2.34 %
Melon	370	540	2400	2.72 %
Orange	190–250	390	1400	6.43 %
Potato	120–240	300–490	610–980	5.38 %
Cucumber	470	700	2900	5.08 %
Pear	180–240	–	2400–3700	1.91 %
Sweet pepper	750	1300	2350	1.07 %
Banana	–	–	–	4.49 %
Beetroot	740	1130	2000	5.97 %
Mushroom	1700	6100	16,000	5.97 %
Tomato	280	350	1700	0.78 %
Grape	85–120	–	–	6.08 %
Carrot	590	960	2250	4.43 %

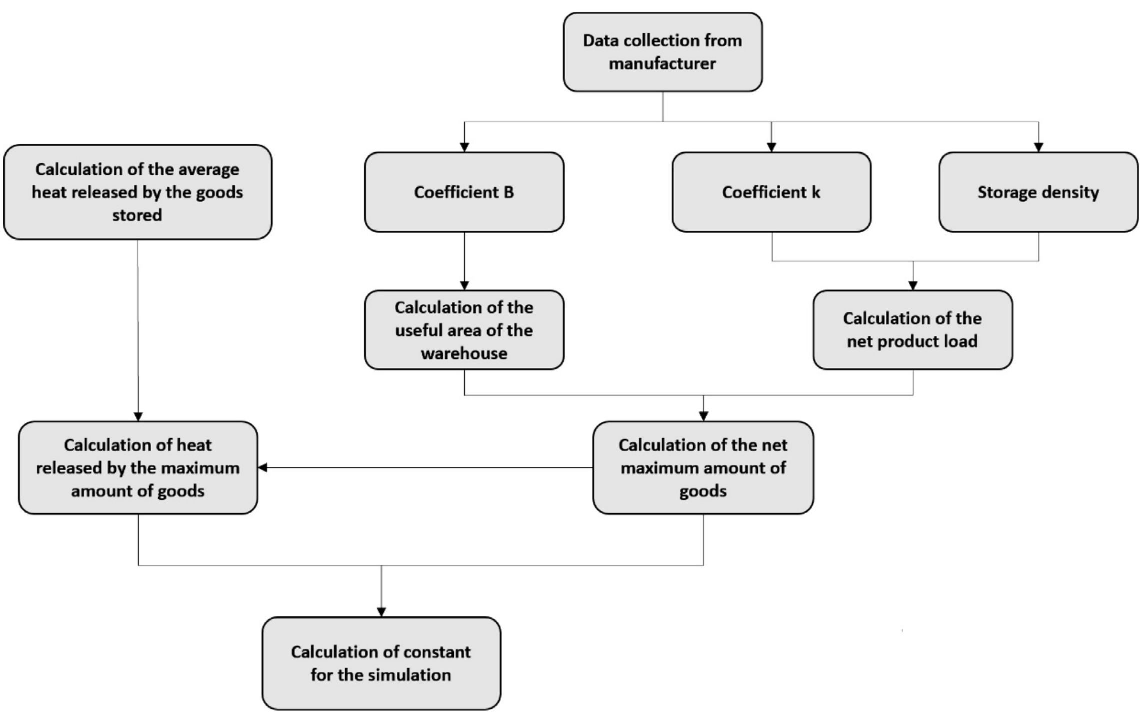

Fig. 8. The steps followed to calculate the constant of the thermal load generated by the goods.

First of all, it is necessary to obtain the average heat released by the goods, AHRG. For this purpose, the values included in Table 4 [21] are used. The last column of Table 4 represents the space in the warehouse set aside for each product annually and based on the space occupied by each type of perishable good (e.g. Celery occupied a 4.32 % area of all storage goods in a standard year). These values have been obtained from the annual report provided by the company month by month during the year of study.

The second step to obtain the average heat released by the goods is to estimate the amount of goods (in kg) that can be stored in the warehouse, which depends on:

- The area occupied by each good (a) and.
- Their stored density (b).

To calculate (a), it is necessary to know the Useful Area of the Warehouse (UAW). This is the space available for storing goods, and it is equal to the total area of the facility minus the space needed

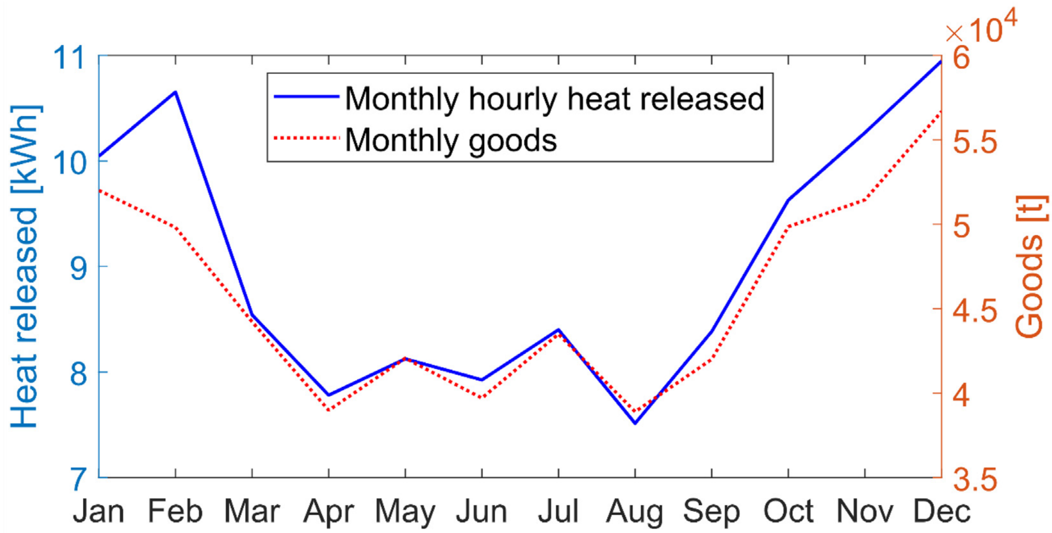

Fig. 9. Monthly heat released by the goods stored in the warehouse.

for elements like the machinery used by employees. Coefficient B (see Fig. 8 and equation (1)) represents this space for machinery. Its value equals 0.85 and it has been provided by the managers of the warehouse. To gauge the UAW, equation (1) is applied.

To calculate (b), two coefficients are needed: the first one represents the gross product load (GPL), which means the storage density, or the maximum quantity of goods that can be stored per square meter and the coefficient $k_{storage}$ = 0.7 (given by the warehouse managers), considering storage height. According to storage regulations for perishable products, the storage density GPL = 448. 25 kg·m^{-2}, and it is computed using equation (2).

To calculate the gross product load, equation (2) is used.

$$UAW\left[m^2\right] = TAW\left[m^2\right]\cdot B \quad (1)$$

$$NPL\left[kg\,m^{-2}\right] = GPL\left[kg\,m^{-2}\right]\cdot \mathrm{k_{storage}} \quad (2)$$

where

- UAW is the Useful Area of the Warehouse.
- TAW is the Total Area of the Warehouse.
- NPL is the Net Product Load.
- GPL is the Gross Product Load.
- $k_{storage}$ represents the density of storage considering the storage height.

In this way, the useful area of the warehouse is 10,400 m^2, and the net product load using equation (2) equals 313 kg/m^2.

$$NMAG[kg] = UAW\left[m^2\right]\cdot \mathrm{NPL}\left[\mathrm{kg\,m^{-2}}\right] \quad (3)$$

where

- NMAG is the net maximum amount of goods.

Computing UAW and NPL in Equation 3, the net maximum amount of goods (NMAG) possible to store in the warehouse equals 3,255,200 kg.

The former value allows us to estimate the heat released by the maximum possible goods stored in the warehouse by multiplying NMAG by the average heat released by the goods (AHRG), following equation (4).

$$HRMAG[W] = AHRG\ \left[W\,kg^{-1}\right]\cdot \mathrm{NMAG}\ [\mathrm{kg}] \quad (4)$$

$$k_{goods}\ \left[W\,kg^{-1}\right] = \frac{HRMAG[W]}{NMAG[kg]} \quad (5)$$

where

- HRMAG is the Heat Released by the Maximum Amount of Goods.
- AHRG is the Average Heat Released by the Goods.

As a result of equation (4), HRMAG = 4.74 kW.

Finally, as a result of equation (5), for the constant $k_{goods,}$ which means the power released per kilogram of goods, an average value of 0.1437 W·kg^{-1} is obtained.

In addition to the heat released by the goods, the monthly hourly average of heat released by the stored goods is calculated and shown in Fig. 9. The obtained values will be introduced later in an internal "Forcing Function" in TRNSYS® and connected to the element "Multizone Building" (Type56 of TRNBuild®) as input for internal gains.

6.2. Air infiltrations

To calculate air infiltrations, it is worth mentioning the two types of air infiltrations that have been considered in this work. The first one takes place before the truck is parked at the dock, which is completely open, and the second one takes place once the truck is parked. There are small gaps between the dock and the back of the truck through which air passes. To estimate the monthly average air infiltrations, it is necessary to consider several parameters:

- The time the truck is parked is around 2 min and 47 secs, t_p.
- The time spent loading or unloading one pallet is 53 secs, $t_{l/u}$.
- The number of trucks that arrive to the warehouse daily is 387 in peak season and 239 in low season, a_t. As was mentioned in Section 3.3, the average is 313 trucks per day.
- The area of each dock is 8.6 m^2, a_d, and the gap through which air passes in the non-hermetic dock during loading and unloading is 0.34 m^2, $a_{l/u}$.

Once these factors are known, the constant is calculated using equations 6 and 7:

$$k_{parking}\left[m^2\cdot \sec\cdot h^{-1}\right] = a_t\left[trucks\cdot hour^{-1}\right]\cdot t_p[\sec]\cdot a_d\left[m^2\right] \quad (6)$$

$$k_{l/u}\left[m^2 \cdot \sec \cdot h^{-1}\right] = n_p\left[pallets \cdot hour^{-1}\right] \cdot t_{l/u}[\sec] \cdot a_{l/u}\left[m^2\right] \quad (7)$$

Sometimes, this information is confidential. For modelling purposes, only average or estimated values are necessary. The flow rate of air infiltrations is calculated by multiplying the monthly constant, entered in TRNSYS® by an internal "Forcing Function" (Type 14), correlated by wind velocity, which is computed with the "ENERGYPLUS WEATHER FILES (EPW)" Type 15 in TRNSYS®. The monthly constant has been estimated following the procedure previously described. A correlation is obtained between wind speed and thermal load due to air infiltration in the storage area, as shown in equation 8.

$$\dot{q}\left[\frac{m^3}{h}\right] = k_{\inf iltrations}\left[\frac{m^2 \cdot \sec}{h}\right] \cdot v_{wind\_\inf iltrations}\left[\frac{m}{\sec}\right] \quad (8)$$

During the adjustment process, several combinations of $k_{infiltrations}$ were checked (see Table 5), but only one constant profile was chosen for the simulations. See Fig. 10 for the thermal load generated by the different air infiltration profiles. To calculate the profiles of the constants of the rejected $k_{inflitrations}$, the parameters used to calculate the rate of air infiltrations has been replaced with values considered acceptable by the company because, according to the workers, both times for parking ($t_{p,}$) and load/unloading one pallet ($t_{l/u}$) are accurate. The difference between real and simulated energy use differs by only 6.75 %.

6.3. Other internal gains: lighting, workers and machinery

Besides the two most important sources of consumption described, there is another internal thermal gain to be considered and included in the model. It includes lighting, workers and machinery.

Light consumption was calculated by considering that the total electrical power installed per square metre is roughly 2 $W \cdot m^{-2}$, but it only works in places where goods are stored. The occupied area of the warehouse was calculated by averaging the daily number of loaded and unloaded pallets. Once this value was obtained, it was multiplied by the total electric power previously calculated to get the thermal load of lighting.

The procedure to calculate the internal gains caused by workers is similar. The maximum number of workers in the warehouse was used. According to the standard, [22] the metabolic heat gain from this kind of worker is 415 W. Knowing this value and the number of workers per hour in the warehouse, the thermal load from the workers was calculated.

Finally, the machinery involved in moving the pallets averages 2 kW according to the datasheet. This is affected by a coefficient of 0.2 to convert it into a thermal load. To calculate the thermal load, it is worth noting that half of the machinery is normally working at the same time.

Once the three additional sources of thermal gains were estimated, they were represented in Fig. 11.

As depicted in Fig. 11, the internal thermal loads are lower in the summer months, and they increase in the winter months. One important detail is that the lights are only on when the pallets are under them, so consumption decreases when there are fewer goods stored in the warehouse (see Section 3.3). The thermal loads of workers and machinery are also lower in the warmer months.

Fig. 12 depicts a Pareto chart showing how the influence of these internal gains in warehouse energy needs is insignificant. The total thermal load generated by machinery, workers and lighting accounts for only 2.20 % of total energy use, while the influence of the thermal losses through the envelope and the thermal load generated by air infiltrations and the goods stored make up 97.80 % of the total energy consumed.

7. Building model

Once the thermal loads were obtained, the next step was to model and simulate the building. To avoid unnecessary work, a simulation with a non-D model was carried out. If the validation of this first model with real data is sufficiently accurate (with a difference from real energy use data of less than 10 %), the model can be accepted, and no more work is needed. If not, a 3D model must be developed using SketchUp®, as explained below.

There are several software packages to model building envelopes. After reviewing the literature, TRNSYS® software was chosen based on researcherś opinions about the suitability of its software for building energy modelling, TRNBuild®. At the beginning of the modelling, the non-D version might be sufficient, without any 3D design software necessary. An energy model can be created directly by entering the dimensions of the surfaces and the orientation of each part of the thermal envelope along with the layers that comprise it. However, due to the complexity of the real scenario to be modelled, the inaccuracy of the initial results could serve as a warning that 3D design software should be used. In this case, the 3D design software called SketchUp® could be selected to create a geometric model to develop an energetic model. The use of SketchUp® software has resulted in the warehouse model depicted in Fig. 13.

SketchUp® has several advantages that make it a good alternative. For instance, its interface is intuitive and easy to learn. It is relatively inexpensive, and it also has a plugin to create thermal zones that can export the geometric model to TRNSYS® more easily.

Once the geometric model has been made in SketchUp®, it is exported to TRNSYS®, where a new project is created using the modelled building (".idf" file) from SketchUp®. At this point, some interesting aspects must be mentioned for proper modelling and a better understanding of the procedure followed in this work.

Table 5
Values used for constant $k_{infiltrations}$ for the different cases analysed, in $m^2 \cdot sec \cdot h^{-1}$.

	Optimal Case	Case 1	Case 2	Case 3
January	29,918.39	36,559.19	59,918.39	17,359.19
February	29,986.04	36,593.02	59,986.04	17,393.02
March	18,951.16	18,475.58	34,551.16	12,475.58
April	18,866.30	18,433.15	34,466.30	12,433.15
May	18,904.71	18,452.35	34,504.71	12,452.35
June	18,882.43	18,441.22	34,482.43	12,441.22
July	18,935.42	18,467.71	34,535.42	12,467.71
August	18,836.61	18,418.31	34,436.61	12,418.31
September	18,933.50	18,466.75	34,533.50	12,466.75
October	29,872.13	36,536.06	59,872.13	17,336.06
November	29,943.27	36,571.63	59,943.27	17,371.63
December	30,018.81	36,609.40	60,018.81	17,409.40

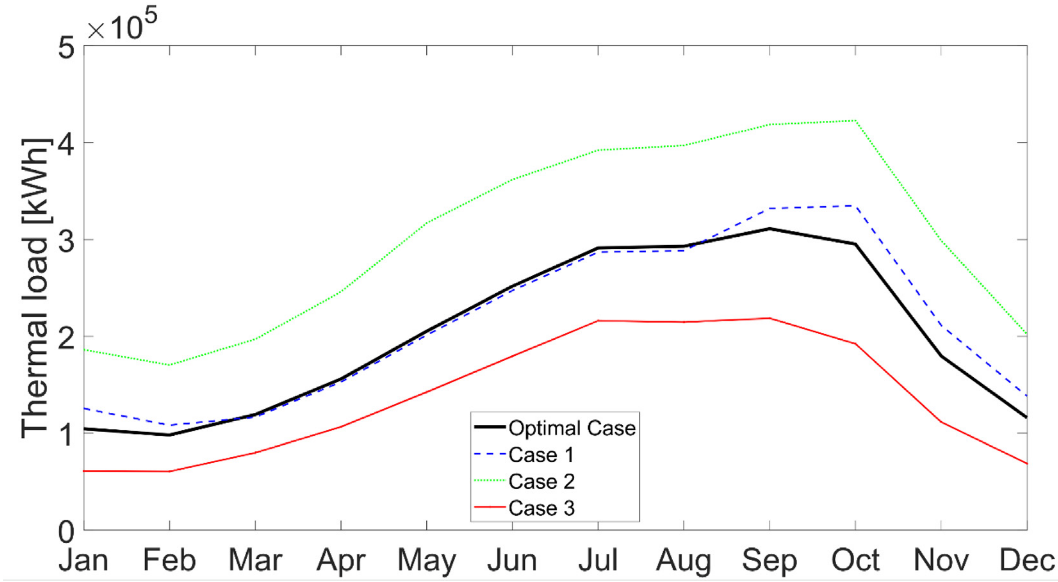

Fig. 10. Thermal load for each case of air infiltration rate analysed.

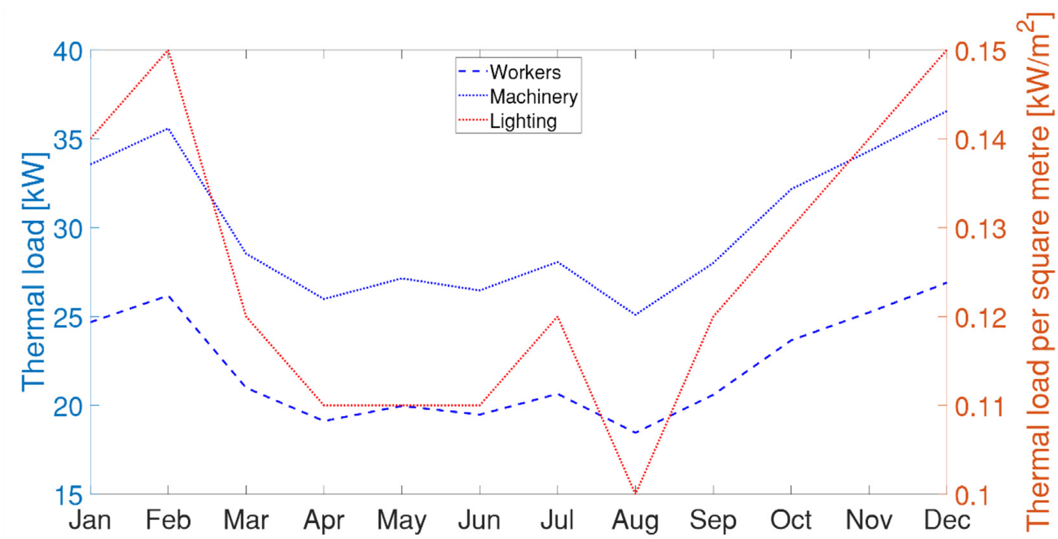

Fig. 11. Thermal load generated by other internal gains.

This building has two different temperature zones and a communication chamber between them, with 21 independent cooling coils in total (as Fig. 5 shows). Thanks to the 3D model, it is possible to locate each coil inside the building. The 3D model also provides the possibility to set the thermal loads received in each cooling coil independently.

7.1. Implementation in TRNSYS®

Once every factor has been estimated and introduced in TRNSYS®, the model is ready to simulate the thermal performance of the building. The results are shown in the next section.

Previous to the simulation, some basic settings need to be established in the software. There are two basic settings: the simulation time, which is a calendar year, and the simulation time step, which is one hour. The remaining settings are established by default. The final version of the model in TRNSYS® is presented in Fig. 14.

The boundary conditions imposed on the model are the following:

- **Environmental conditions** of the climatic working area closest to the warehouse. These conditions were recorded every 15 min. The weather data was taken from the meteorological database, Meteonorm in TRNSYS®.

- **Required Internal conditions** for adequate storage of the products. Two storage zones were considered, zone 1 chamber at 4 °C and zone 2 chamber at 8 °C. Four differentiated refrigeration zones were modelled with SketchUp®: the 4 °C chamber, the 4 °C loading and unloading antechambers and the 8 °C chamber.

- **Internal thermal loads from stored goods, infiltration, machinery, workers, etc.** Conditions, quantity, thermal characteristics, the time the goods were not refrigerated during the loading/unloading process, the characteristics of the dock, etc., see Section 6.

In the case of the 3D model, the location of each cooling coil was imposed as a boundary condition. In this way, it is possible to locate each coil inside the building, and the 3D model provides

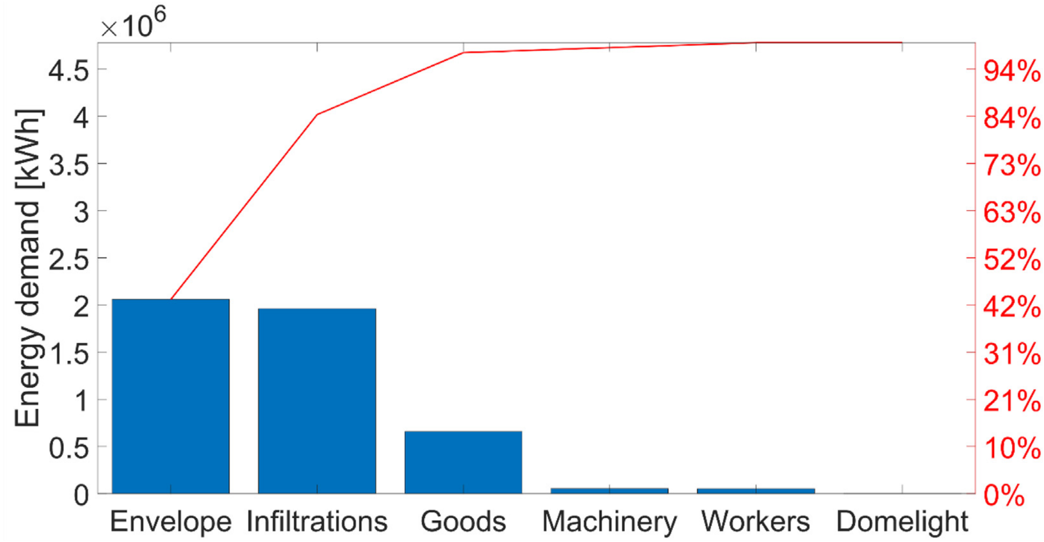

Fig. 12. Pareto chart for the different thermal loads.

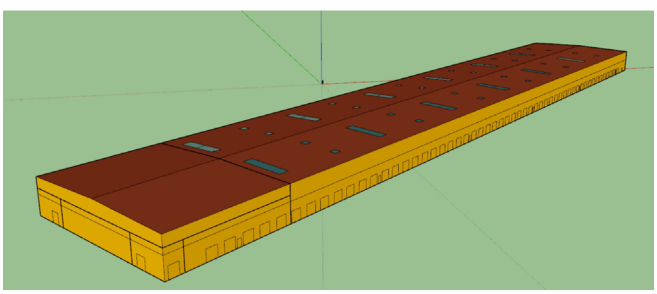

Fig. 13. Geometric model of the warehouse in SketchUp®.

the possibility to set different thermal loads received by each cooling coil independently. With the information of each cooling coil and the different loads based on the orientation of the building, a better adjustment of the overall energy consumption data was obtained than that of the non-D model.

8. Results and discussion

In section 6, we said that the thermal loads generated by air infiltrations and the goods have a great impact on the warehouse's energy needs. In fact, according to the results obtained from the simulations, these factors combined account for 65 % of the average monthly energy consumption of the warehouse. Fig. 15 shows the influence of air infiltrations and the heat released by the goods.

However, considering the influence of each factor individually is even more remarkable. According to the simulations, the thermal load caused by air infiltrations contributes 47 % to monthly energy use, while the thermal load for goods is 18 %. This clearly shows the value of modelling these two factors as accurately as possible, as well as controlling them to reduce energy consumption in the warehouse.

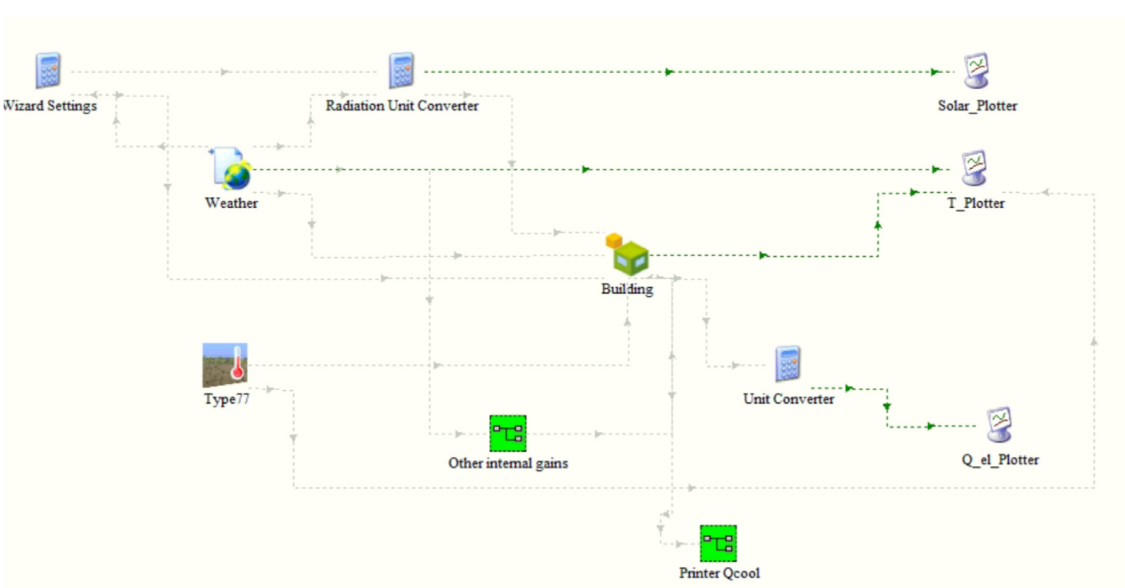

Fig. 14. TRNSYS® simulation sketch.

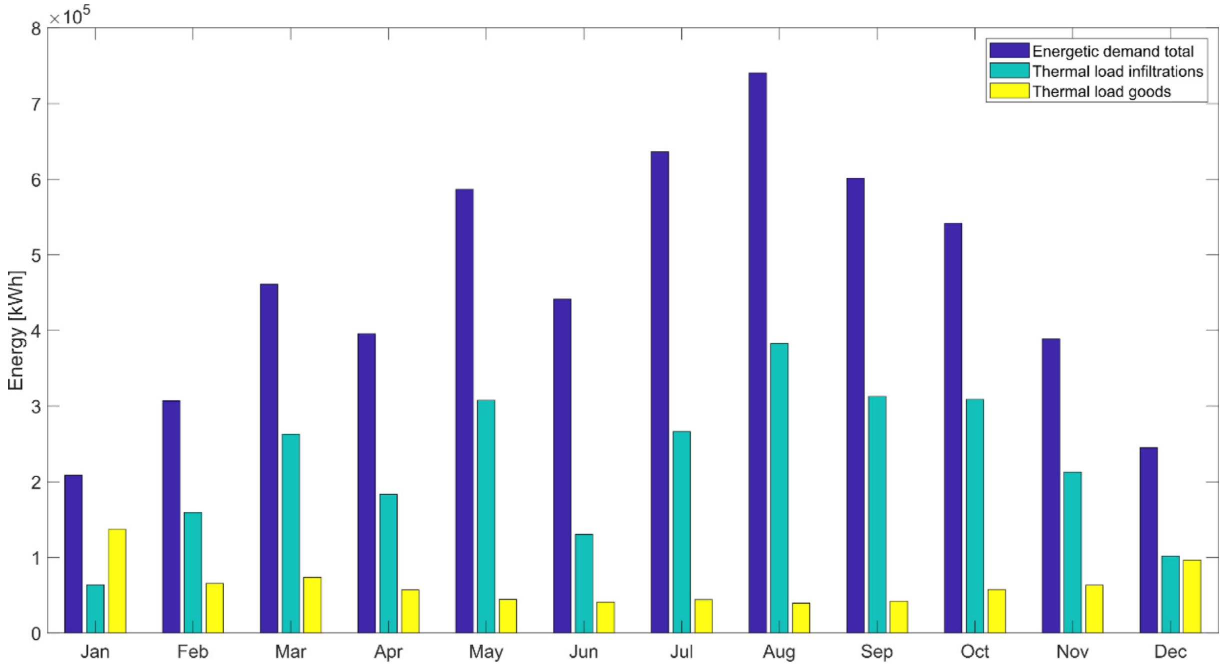

Fig. 15. Influence of the air infiltrations and heat released by the goods in the energy needs of the warehouse.

As was mentioned at the beginning of the previous section, there are two possible energy models: one created without any 3D design and one using a 3D design. The first is referred to as the non-D model, and the second one, the 3D model.

The most relevant results of the simulations are shown in Fig. 16. Taking into account that both models have the same values for all the internal thermal gains, it can be seen how there is significantly less difference between the 3D and real data charts than between the non-D model and real data.

These differences are expressed in percentages in Fig. 17. The monthly average difference between the 3D model and the real data is 7.22 %, while the difference between the non-D model and the real data is 26 %. During autumn, winter and spring, the errors are close to 0 %, while during June, July and August, the error fluctuates. This is due to the large differences in temperature between the outside environment and the refrigerated warehouse. Infiltrations become a more important factor during the summer. A special study of the times, schedule and number of loading/unloading processes during these months could improve the detailed model of infiltrations during this period.

Most of the uncertainties involve thermal loads due to infiltrations. To be more accurate, the infiltration model needs to have well-detailed boundary conditions (instantaneous environmental data and, overall, the areas of infiltration and the exact loading and unloading times for each operation must be well-defined).

Fig. 18 shows the comparison of instantaneous thermal energy consumption during a week between:

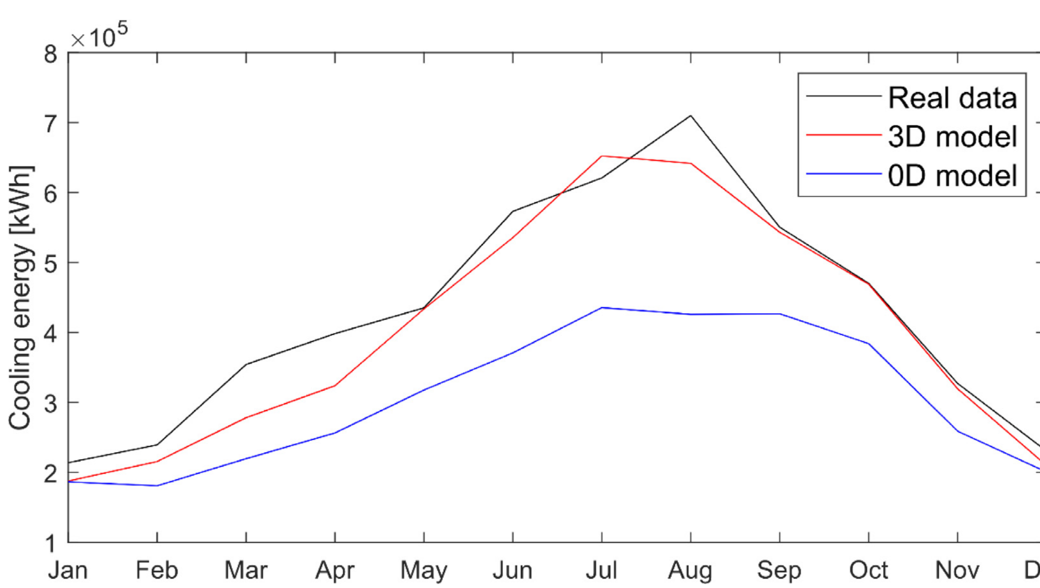

Fig. 16. Comparison between the 3D(red) and non-D(blue) models and real data (black). (For interpretation of the references to colour in this figure legend, the reader is referred to the web version of this article.)

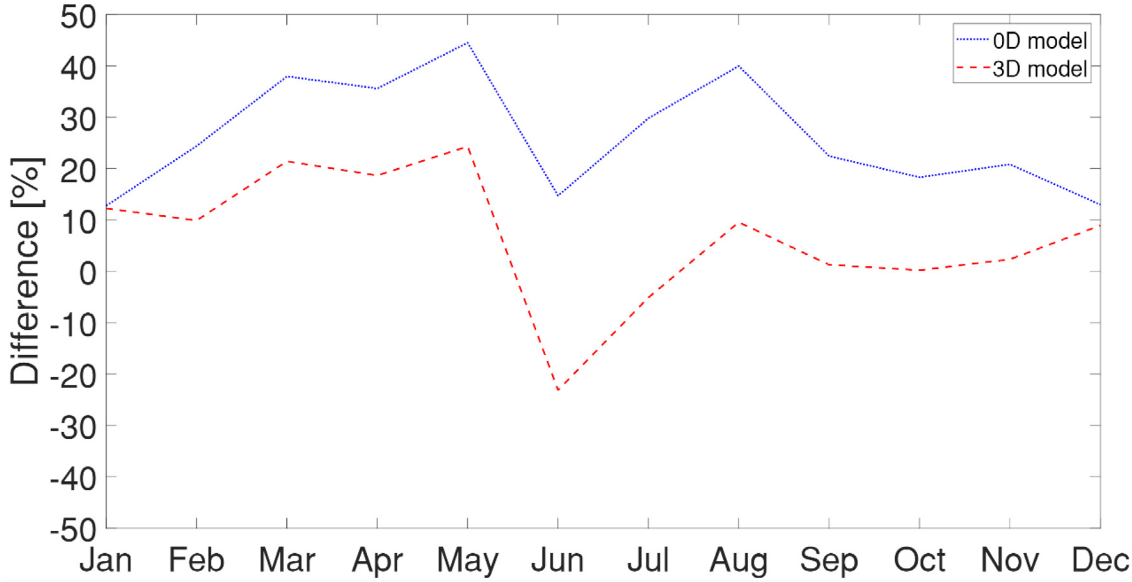

Fig. 17. Percentage of monthly differences between 3D and non-D models compared to real energy demand.

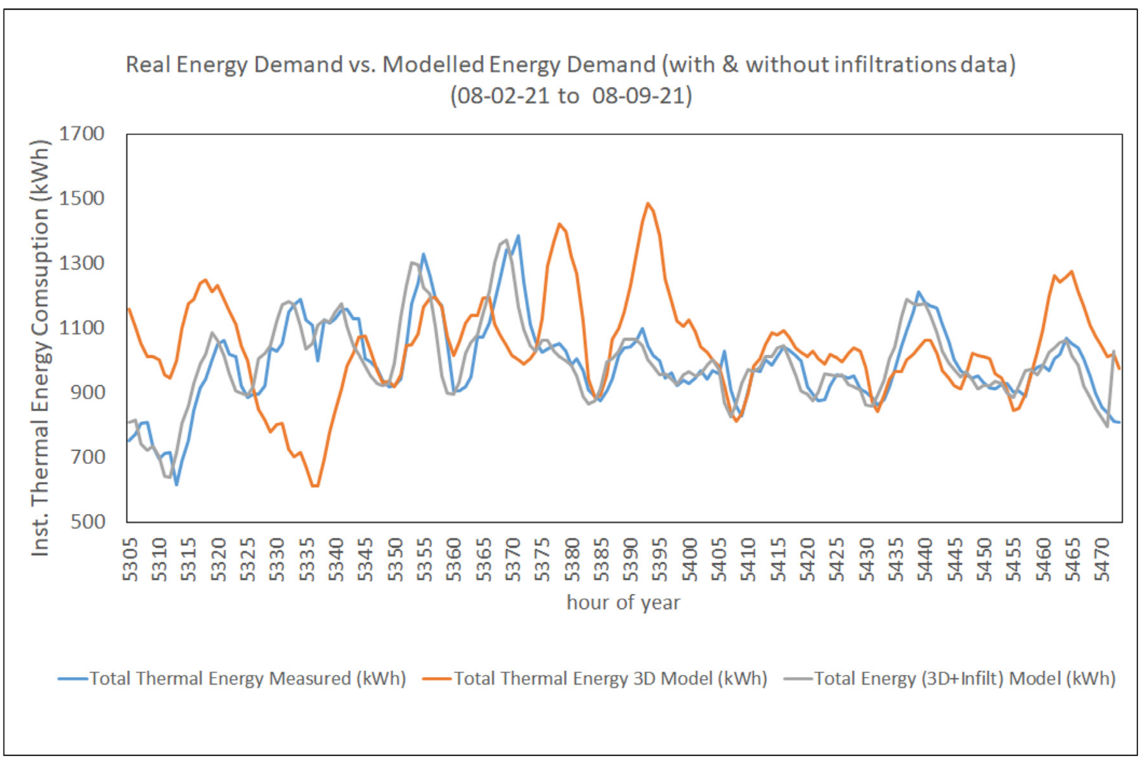

Fig. 18. Comparison between actual values and 3D model with/without actual data values due to infiltrations.

- Measured data (blue),
- 3D-modelled data for a whole year (orange) and
- 3D-modelled data with real, instantaneous data on (grey): (i) controlled, measured infiltration demand, (ii) environmental data (external temperature, humidity, etc.) and (iii) instantaneous internal thermal demand (goods, machinery, etc.) imposed as boundary conditions. This data was collected during a campaign to measure the infiltrations of the warehouse (times of loading/unloading processes, velocity of air mass flows in/out of the warehouse, etc.), exhaustive control of stored goods and, of course, with real, measured environmental data.

It is possible to see that the accuracy of the model is very high when the infiltration contribution to the demand is the correct one.

These boundary conditions are almost impossible to be measured in a real installation during a whole year and, in addition, the capacity of the model to evaluate possible improvements over the system (e.g., increase envelope insulation) will be reduced because of the constrictions of the modelled scenario. But detailed modelling of the thermal demand due to infiltration, and its possible correlation with easily measurable parameters such as instantaneous wind velocity, open a future line of work for researchers.

Another drawback when addressing the cooling system power design is the uncertainty when measuring internal thermal loads due to operational processes. These thermal loads may not be considered as important as the building envelope in the first step, which is a major mistake. However, there are few works incorporating methodologies to guide users on how to quantify these thermal loads and validate the results in the timespan of one year.

The value of simulation, which has been clearly presented in the literature review, supports decision-makers when assessing the behaviour of a building or when improving the envelope, which implies an investment. On occasions, to avoid the risks involved in uncertain data, the investment is not carried out or, if it is, the outcome is not as profitable as expected or, in the worst case, it produces unexpected losses. Some researchers could be concerned about these incomprehensible discrepancies without suspecting that the answer may be found in a basic modelling of the envelope using TRNSYS®.

The main essence of this work is to give guidance when modelling a complex, highly uncertain scenario, like the one illustrated in this paper. First of all, it should be noted that identifying the main sources of consumption is a requirement. To achieve this goal, users must be aware of the differences when modelling with the basic elements of TRNSYS® or when more sophisticated work is conducted when modelling the building envelope. Daily operational processes may have deeper and unexpected impacts on the thermal loads than the building envelope. Although the calculation is cumbersome, this research has illustrated that the impact on the final result is unquestionable.

9. Conclusions

This study exemplifies how a large building with complex daily processes can be modelled to simulate thermal performance. With this aim, annual energy simulations for non-D and 3D (Sketchup® and TRNSYS®) models were carried out. Previous to performing the simulations, a methodology and procedure to estimate the thermal loads of different goods were provided to support the researchers and practitioners. To check the robustness of the developed model, the results of the simulations were validated using real data for one year.

Several significant findings have resulted from this study. One of the most remarkable aspects of this kind of modelling is to resolve the quandary between user-friendliness and accuracy. When the objectives are to obtain basic results and be easy to use, non-D software is recommended. Moreover, the workload involved in modelling a building in non-D is considerably less. As has been demonstrated by the simulations, when more exact results are needed, a geometric model using 3D design software should be developed and then exported to create the energetic model.

As it was shown in Section 6, the 3D model reduces the difference from the real data by 19 %, going from 26 % for the non-D model to 7.22 %.

The possibility of modifying the thermal load profiles calculated following the procedure explained here increases the value of this kind of modelling. This method has demonstrated optimal results and has shown that it is possible to decrease energy consumption by simply changing some parameters of the loading/unloading processes.

Another important conclusion is that by means of the proposed modelling and methodology, a more reliable assessment of possible investments, projects and/or actions to improve thermal efficiency in an existing building are possible. In addition, the methodology is useful to calculate the necessary thermal demand of a similar warehouse under construction or in the design phase and therefore, to adjust the investment for the HVAC system.

To obtain a detailed model of energy consumption due to infiltrations, a record of loading/unloading processes with times, schedule and goods should be made available.

As a result of our findings, some guidelines can be provided to increase companies' competitive advantage by reducing energy consumption and decreasing CO2 emissions, contributing to SDG7. By modelling the facility, major sources of consumption were identified. The most important of these was infiltration of air from the docks, accounting for 47 % of the total energy consumed and the energy required by the goods, accounting for 18 %. The implications for managers are focused on enhancing operational procedures for workers when loading and unloading. This includes controlling the time when the docks are open and improving infrastructures to seal the gaps between trucks and the dock.

As future works and usefulness of the described model is possible to say that: the 3D model and methodology could be used during the design phase for new buildings to optimise the placement of each cooling coil; to calculate the power of HVAC System; to decide the correct isolation, etc. The modelling of different preconstruction scenarios (building location, expected climate, expected internal loads, type and quality of the envelope, etc.) would be possible following the described methodology. As well as the adaptation to possible internal and external thermal situations to which the building may be subjected and the response that the installed refrigeration equipment may have in a quick way and with average values close to reality.

The clear limitation of the described model is the inability to obtain detailed results for specific points of the building, as temperature values, wind velocity, thermal loads due to infiltration or other fluid dynamics parameters. The model is designed for the response of global thermal loads differentiated by zones (or defined areas of the building) and is not intended to be a CFD model. This limitation becomes an advantage when it is compared its calculation time versus CFD models and with its quick adaptation to different scenarios. While with CFD models it is necessary to prepare detailed meshes with millions of cells to obtain useful results for each scenario, with this model its only necessary to define correctly the boundary conditions.

The described model can offer a global calculation of building's thermal loads of any one of the zones the designer may consider. And also, it́s possible to use the results given by the model in order to select the HVAC equipment and its performance; to optimise the power required; and/or to evaluate the amortisation of different energy retrofitting actions on the building.

CRediT authorship contribution statement

F. Vera-García: Conceptualization, Methodology, Formal analysis, Investigation, Supervision, Writing – review & editing. **J.J. Rubio-Rubio:** Data curation, Software, Validation, Writing – original draft. **A. López-Belchí:** Formal analysis, Validation, Investigation, Writing – review & editing. **E. Hontoria:** Data curation, Resources, Writing – review & editing.

Data availability

No data was used for the research described in the article.

Declaration of Competing Interest

The authors declare that they have no known competing financial interests or personal relationships that could have appeared to influence the work reported in this paper.

Acknowledgements

This research was funded by RTI2018-099139-B-C21 from Ministry of Science and Innovation - National Research Agency (MCIN/AEI) 10.13039/501100011033 and by "ERDF A way of making Europe" of the "European Union".

References

[1] Directive 2010/31/EU of the European Parliament and of the Council of 19 May 2010 on the energy performance of buildings, Official Journal of the European Union. http://data.europa.eu/eli/dir/2010/31/oj last access 2022/04/20.

[2] M.J. Laustsen, Energy efficiency requirements in building codes, energy efficiency policies for new buildings (IEA Information paper In Support of the G8 Plan of Action), International Energy Agency.https://iea.blob.core.windows.net/assets/3783f5e8-b14c-4c18-b04c-aab7c59d6e92/Building_Codes.pdf last access 2022/04/20.

[3] A. Hepbasli, Low exergy (LowEx) heating and cooling systems for sustainable buildings and societies, Renew. Sust. Energ. Rev. 73 (2012) 104–116, https://doi.org/10.1016/j.rser.2011.07.138.

[4] M. Kharseh, L. Altorkmany, M. Al-Khawaj, F. Hassani, Warming impact on energy use of HVAC system in buildings of different thermal qualities and in different climates, Energy Convers. Manag. 106 (2014) 111–181, https://doi.org/10.1016/j.enconman.2014.02.001.

[5] M. Webb, L. Aye, R. Green, Simulation of a biomimetic façade using TRNSYS, Appl. Energy 670 (2018) 694–1213.

[6] E. Massaguer, A. Massaguer, L. Montoro, J.R. Gonzalez, Development and validation of a new TRNSYS type for the simulation of thermoelectric generators, Appl. Energy 134 (2014) 65–74.

[7] B. Quesada, C. Sánchez, J. Cañada, R. Royo, J. Payá, Experimental results and simulation with TRNSYS of a 7.2kWp grid-connected photovoltaic system, Appl. Energy 88 (5) (2011) 1772–1783.

[8] M.-A. Kenai, L. Libessart, S. Lassue, D. Defer, Impact of green walls occultation on energy balance: development of a TRNSYS model on a brick masonry house, J. Build. Eng. 44 (2021) 102634.

[9] F. Eddib, M.A. Lamrani, S. Ait bouyahia, TRNSYS validation of a study on building's energetic evaluation in north of morocco, Energy Procedia 139 (2017) 334–339.

[10] P. Potočnik, B. Vidrih, A. Kitanovski, E. Govekar, Analysis and optimization of thermal comfort in residential buildings by means of a weather-controlled air-to-water heat pump, Build. Environ. 68 (2018) 79–140, https://doi.org/10.1016/j.buildenv.2018.05.044.

[11] I. Sarbu, C. Pacurar, Experimental and numerical research to assess indoor environment quality and schoolwork performance in university classrooms, Build. Environ. 141–154 (2015) 93, https://doi.org/10.1016/j.buildenv.2015.06.022.

[12] J.P. Delgado Marín, F. Vera García, J.R. García Cascales, Use of a predictive control to improve the energy efficiency in indoor swimming pools using solar thermal energy, Sol. Energy 380 (2019) 390–1179, https://doi.org/10.1016/j.solener.2019.01.004.

[13] D. Delcroix, M. Kummert, A. Daoud, Development and numerical validation of a new model for walls with phase change materials implemented in TRNSYS, J. Build. Perform. Simul. 422 (2017) 437–1410, https://doi.org/10.1080/19401493.2017.1280087.

[14] M. Villa-Arrieta, A. Sumper, A model for an economic evaluation of energy systems using TRNSYS, Appl. Energy 765 (2018) 777–1215, https://doi.org/10.1016/j.apenergy.2018.02.045.

[15] D. Brough, J. Ramos, B. Delpech, H. Jouhara, Development and validation of a TRNSYS type to simulate heat pipe heat exchangers in transient applications of waste heat recovery, Int. J. Thermofluids (2020) 100056–100059, https://doi.org/10.1016/j.ijft.2020.100056.

[16] S. Bordignon, G. Emmi, A. Zarrella, M. De Carli, Energy analysis of different configurations for a reversible ground source heat pump using a new flexible TRNSYS Type, Appl. Therm. Eng. (2021) 117413–1117197, https://doi.org/10.1016/j.applthermaleng.2021.117413.

[17] C.P. Kurian, S. Milhoutra, V.I. George, Sustainable building design based on building information modeling (BIM). IEEE International Conference on Power System Technology (POWERCON), 2016; 1:6, doi: 10.1109/POWERCON.2016.7754039.

[18] S. Chang, D. Castro-Lacouture, F. Dutt, Y.P. Pei-Ju, Framework for evaluating and optimizing algae façades using closed-loop simulation analysis integrated with BIM, Energy Procedia. 237 (2017) 244–1143, https://doi.org/10.1016/j.egypro.2017.12.677.

[19] A. Sporr, G. Zucker, R. Hofmann, Automatically creating HVAC control strategies based on building information modeling (BIM): heat provisioning and distribution, Energies (2020) 4403–4413, https://doi.org/10.3390/en13174403.

[20] A. Mohanta, S. Das, M.R. Narayan, Building envelope trade-off method integrated with BIM-based framework for energy-efficient building envelope, Archit. Eng. Des. Manag. 516 (2021) 536–1517, https://doi.org/10.1080/17452007.2021.1941741.

[21] 2018 ASHRAE handbook: Fundamentals. Atlanta, GA: American Society of Heating, Refrigeration and Air-Conditioning Engineers.

[22] UNE-EN ISO 8996:2021. Ergonomics of the thermal environment – Determination of metabolic rate.